Laser with an in-loop relative frequency stability of 1.0×10^{-21} on a 100-ms time scale for gravitational-wave detection

F. Acernese,[1,2] M. Alshourbagy,[3,4] F. Antonucci,[5] S. Aoudia,[6] K. G. Arun,[7] P. Astone,[5] G. Ballardin,[8] F. Barone,[1,2] L. Barsotti,[3,4] M. Barsuglia,[9] Th. S. Bauer,[10] S. Bigotta,[3,4] S. Birindelli,[6] M. A. Bizouard,[7] C. Boccara,[11] F. Bondu,[6,*] L. Bonelli,[3,4] L. Bosi,[12] S. Braccini,[3] C. Bradaschia,[3] A. Brillet,[6] V. Brisson,[7] H. J. Bulten,[10,13] D. Buskulic,[14] G. Cagnoli,[15] E. Calloni,[1,16] E. Campagna,[15,17] B. Canuel,[8] F. Carbognani,[8] L. Carbone,[12] F. Cavalier,[7] R. Cavalieri,[8] G. Cella,[3] E. Cesarini,[15,18] E. Chassande-Mottin,[9] S. Chatterji,[5] F. Cleva,[6] E. Coccia,[19,20] J. Colas,[8] M. Colombini,[5] C. Corda,[3,4] A. Corsi,[5] F. Cottone,[12,21] J.-P. Coulon,[6] E. Cuoco,[8] S. D'Antonio,[19,20] A. Dari,[12,21] V. Dattilo,[8] M. Davier,[7] R. De Rosa,[1,16] M. Del Prete,[3,22] L. Di Fiore,[1] A. Di Lieto,[3,4] M. Di Paolo Emilio,[19,23] A. Di Virgilio,[3] V. Fafone,[19,20] I. Ferrante,[3,4] F. Fidecaro,[3,4] I. Fiori,[8] R. Flaminio,[24] J.-D. Fournier,[6] S. Frasca,[5,25] F. Frasconi,[3] L. Gammaitoni,[12,21] F. Garufi,[1,16] G. Gemme,[26] E. Genin,[8] A. Gennai,[3] A. Giazotto,[3,8] M. Granata,[9] V. Granata,[14] C. Greverie,[6] G. Guidi,[15,17] H. Heitmann,[6] P. Hello,[7] S. Hild,[27] D. Huet,[8] P. La Penna,[8] M. Laval,[6] N. Leroy,[7] N. Letendre,[14] M. Lorenzini,[15,18] V. Loriette,[11] G. Losurdo,[15] J.-M. Mackowski,[24] E. Majorana,[5] N. Man,[6] M. Mantovani,[8] F. Marchesoni,[12,21] F. Marion,[14] J. Marque,[8] F. Martelli,[15,17] A. Masserot,[14] F. Menzinger,[8] C. Michel,[24] L. Milano,[1,16] Y. Minenkov,[19,20] S. Mitra,[6] M. Mohan,[8] J. Moreau,[11] N. Morgado,[24] A. Morgia,[19,20] S. Mosca,[1,16] B. Mours,[14] I. Neri,[12,21] F. Nocera,[8] G. Pagliaroli,[19,20] C. Palomba,[5] F. Paoletti,[3,8] S. Pardi,[1,16] A. Pasqualetti,[8] R. Passaquieti,[3,4] D. Passuello,[3] G. Persichetti,[1,16] F. Piergiovanni,[15,17] L. Pinard,[24] R. Poggiani,[3,4] M. Punturo,[12] P. Puppo,[5] O. Rabaste,[9] P. Rapagnani,[5,25] T. Regimbau,[6] F. Ricci,[5,25] A. Rocchi,[19] L. Rolland,[14] R. Romano,[1,2] P. Ruggi,[8] B. Sassolas,[24] D. Sentenac,[8] B. L. Swinkels,[8] R. Terenzi,[19,20] A. Toncelli,[3,4] M. Tonelli,[3,4] E. Tournefier,[14] F. Travasso,[12,21] J. Trummer,[14] G. Vajente,[4,28] J. F. J. van den Brand,[10,13] S. van der Putten,[10] D. Verkindt,[14] F. Vetrano,[15,17] A. Viceré,[15,17] J.-Y. Vinet,[6] H. Vocca,[12] M. Was,[7] and M. Yvert[14]

[1]*INFN, Sezione di Napoli, 80126 Napoli, Italy*
[2]*Università di Salerno, 84084 Fisciano (Sa), Italy*
[3]*INFN, Sezione di 56127 Pisa, 56127 Pisa, Italy*
[4]*Università di Pisa, 56127 Pisa, Italy*
[5]*INFN, Sezione di Roma, 00185 Roma, Italy*
[6]*ARTEMIS, Observatoire Côte d'Azur, CNRS, Université Nice Sophia Antipolis, 06304 Nice, France*
[7]*LAL, IN2P3/CNRS, Université Paris-Sud, 91198 Orsay, France*
[8]*European Gravitational Observatory (EGO), 56021 Cascina (Pi), Italy*
[9]*APC, CNRS, Observatoire de Paris, CEA, Université Paris VII, 75205 Paris France*
[10]*NIKHEF, NL-1009 DB Amsterdam, The Netherlands*
[11]*ESPCI, 75005 Paris, France*
[12]*INFN, Sezione di Perugia, 06123 Perugia, Italy*
[13]*Vrije Universiteit, NL-1081 HV Amsterdam, The Netherlands*
[14]*LAPP, IN2P3/CNRS, Université de Savoie, Annecy-le-Vieux, 74941 Annecy, France*
[15]*INFN, Sezione di Firenze, 50019 Sesto Fiorentino, Italy*
[16]*Università di Napoli "Federico II," Complesso Universitario di Monte S. Angelo, 80126 Napoli, Italy*
[17]*Università degli Studi di Urbino "Carlo Bo," 61029 Urbino, Italy*
[18]*Università degli Studi di Firenze, 50121 Firenze, Italy*
[19]*INFN, Sezione di Roma Tor Vergata, 00133 Roma, Italy*
[20]*Università di Roma Tor Vergata, 00133 Roma, Italy*
[21]*Università di Perugia, 06123 Perugia, Italy*
[22]*Università di Siena, 53100 Siena, Italy*
[23]*Università dell'Aquila, 67100 L'Aquila, Italy*
[24]*LMA, IN2P3/CNRS, Villeurbanne, 69622 Lyon, France*
[25]*Università "La Sapienza," 00185 Roma, Italy*
[26]*INFN, Sezione di Genova, 16146 Genova Italy*
[27]*University of Birmingham, Birmingham, United Kingdom*
[28]*Scuola Normale Superiore, 56126 Pisa, Italy*

We report on the stabilization of the laser frequency for the Virgo gravitational-wave detector. We have obtained a frequency noise level, measured in loop, of 1.9×10^{-7} Hz/$\sqrt{\text{Hz}}$ at 10 Hz for the 1064 nm laser; this value is limited by shot noise. The Allan standard deviation for relative frequency noise is 1.0×10^{-21} on a 100-ms time scale. The spectral density of the laser frequency noise is negligible in the channel where gravitational waves ought to appear and meets the specifications for the target spectral resolution of the Virgo interferometer in the 10 Hz–10 kHz detection bandwidth.

PACS number(s): 42.60.Da, 04.80.Nn, 06.30.Ft

I. INTRODUCTION

A gravitational wave changes the round-trip time of a photon between two inertial test masses at rest. The round-trip time of photons between spatial coordinates $(0,0,0)$ and $(L,0,0)$ is, to first order in the gravitational-wave amplitude h,

$$\tau = \frac{2L}{c} + \frac{1}{2}\int_0^{2L/c} h_+(t)dt,$$

where $h_+(t)$ is the gravitational wave with a wave vector along the z axis and optimal polarization. A Fabry-Perot cavity resonator converts a gravitational wave into a phase change in the light circulating in the cavity. The suspended mirrors of the optical resonator [1] realize inertial test masses at rest for analysis frequencies above the main pendulum resonant frequency. The Pound-Drever-Hall technique [2,3] is able to measure the phase variation. The laser phase, before entering the cavity, is modulated at a frequency f_{mod}. The nonresonating sidebands provide a reference oscillator. The carrier is resonant, sensing gravitational waves. A photodetector detects the reflected light, beating the sidebands against the carrier; the electrical current is mixed with the f_{mod} signal and low-pass filtered; the resulting signal is proportional to the phase variations due to the gravitational wave.

The Ligo [4] and Virgo [5] gravitational-wave detectors use a laser light of 1.064 μm, 2 kilometric Fabry-Perot cavities in the arms of a Michelson interferometer and an additional upstream power recycling cavity for additional laser power buildup on the beam splitter. The Michelson interferometer output port is tuned on the dark fringe, so that the phase variations from gravitational waves add up on this port. The detection band of the Virgo detector is 10 Hz–10 kHz. Its best achieved resolution spectral density is, in units of the gravitational wave h, $7 \times 10^{-23}/\sqrt{\text{Hz}}$ at 200 Hz. A 140-m-long Fabry-Perot cavity with suspended mirrors, the input mode cleaner, filters out the input beam angular jitter [6]. An independent rigid output cavity selects the TEM00 mode containing the signal.

The signal from the light reflected on the second face of the interferometer splitter compares the *common mode* of the relative motion of the two long optical resonators to the relative laser frequency noise; this is the actual reference for stabilizing the laser frequency. In the following sections we will show that the symmetry of the two long Fabry-Perot resonators, the pole of the recycling cavity, and a feedforward technique provide the needed isolation for the remaining laser frequency noise.

II. SPECIFICATIONS ON A LASER CLOCK FOR A GRAVITATIONAL WAVE TRANSDUCER

The laser frequency noise couples to the dark fringe via the interferometer asymmetries. Let us name F_{asym} the trans-

———————
*bondu@oca.eu

fer function between the laser relative frequency noise and the interferometer dark port, calibrated in units of the gravitational wave h. The specification on the spectral density of the Virgo instrument resolution, divided by the factor F_{asym}, gives the specification on the input laser frequency noise spectral density.

The calculation of the transfer function F_{asym} gives

$$F_{\text{asym}} = \frac{\Delta\mathcal{F}}{\mathcal{F}}\frac{1}{1+if/f_{\text{rec}}} + \frac{\Delta R}{4}\frac{f_P}{f_{\text{rec}}}\frac{1+if/f_P}{1+if/f_{\text{rec}}},$$

where $\mathcal{F}$ is the average finesse of the two cavities, $\Delta\mathcal{F}$ is the finesse difference, ΔR is the reflectivity difference of the two long Fabry-Perot resonators, f_P is the average cavity pole (500 Hz in the Virgo detector), and $f_{\text{rec}} = 8$ Hz is the pole of the (power recycling cavity–average long cavity) compound cavity. The first term of this asymmetry function is the effect of the effective optical path length difference, filtered by the pole of the recycling cavity; the second term, showing the effect of a contrast defect, comes from a full calculation of the field on the dark fringe. The ΔR term is the product of the average cavity gain factor times the difference of the cavity mirror losses. The asymmetry function is measured to be typically 6.4×10^{-4} for $f \gg f_P$. The corresponding interferometer contrast defect is 8×10^{-7}, good enough to relax the specifications on the input laser frequency noise. The specifications on the laser frequency noise are then 4×10^{-6} Hz/$\sqrt{\text{Hz}}$ at 50 Hz and 3×10^{-4} Hz/$\sqrt{\text{Hz}}$ at 10 kHz, to be compared to a free-running laser frequency noise spectral (10 kHz/f) Hz/$\sqrt{\text{Hz}}$. The interferometer symmetry is thus not enough to get rid of the laser frequency noise; feedback loops are necessary.

III. ARCHITECTURE

We show in this section that two different frequency references have to be used, resulting in a complex architecture of laser frequency stabilization.

The only reference stable enough to meet the requirement on the laser frequency at 50 Hz is the common mode of the interferometer. The open loop transfer function of the frequency stabilization of the laser to the common mode [second stage of frequency stabilization (SSFS)] has a bandwidth of 23 kHz; its limit being the 50 kHz free spectral range of the 3 km Fabry-Perot cavities. At 10 kHz, the loop gain of the SSFS loop is only a few units; the laser frequency noise spectral density of the free-running Nd:YAG laser is more than 3 orders of magnitude too large. The laser is thus prestabilized in frequency to the input mode cleaner (first stage of frequency stabilization). This loop has a 300 kHz bandwidth; its limit is the 1 MHz free spectral range of the cavity. The correction signal of the SSFS loop is electronically added to the error point of the prestabilization loop.

The correction signal of the SSFS loop is also used as an error signal to keep the input mode-cleaner cavity at resonance. This loop includes a digital filter whom the delay limits the bandwidth of this loop to 100 Hz.

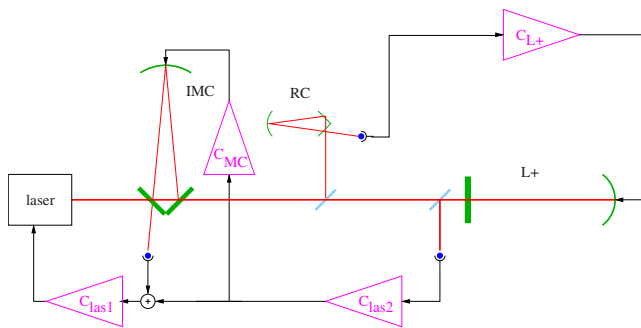A 30-cm-long rigid cavity made out of ULE® (Corning) constitutes the reference for damping the oscillations of the

FIG. 1. (Color online) Laser frequency stabilization in two stages. Semicircled dots are symbols for photodetectors. "IMC" stands for the input mode-cleaner cavity, with suspended mirrors, in vacuum; "RC" stands for the short and rigid 30 cm cavity in vacuum; and "L+" stands for the common mode of the two 3 km cavities. The triangles represent correction filters. The IMC lock filter (C_{IMC}) and the common mode filter (C_{L_+}) are digital filters. The laser is prestabilized to the input mode-cleaner cavity; the second stage of stabilization uses the common mode of the interferometer as a reference.

common mode of the two long Fabry-Perot cavities. This feedback loop has a bandwidth of 1.5 Hz. The thermal noise displacement of the mirror surfaces limits the spectral density of the rigid reference cavity to $\sim 1.0 \times 10^{-2}$ Hz/$\sqrt{\text{Hz}}$ at 100 Hz [7]. The coupling of this noise in the dark fringe is reduced with a feed-forward technique: the reference cavity error signal is filtered and added to the correction signal of the differential mode locking loop. The filter amplitude is identical to the measured transfer function of the reference cavity error signal to the correction signal of the differential mode locking loop (elaborated from the dark fringe signal) and has an opposite sign. The noise in the dark fringe is negligible after an effective reduction of ~ 50 in the 2–80 Hz range.

Figure 1 displays the schematics of all loops together. We have computed the whole open loop transfer function and checked that it is stable, provided that the bandwidths of the various loops are separated by 1 order of magnitude. The individual loops, described above, have integration stages at low frequencies to ensure lock accuracy and enough low frequency noise suppression. We computed the servo loop equations of the whole system when operating in the linear regime. We studied the transfer function between each noise source (readout noises, digitization noises, amplifiers voltage noises, free-running laser noise, and residual motion of the suspended mirrors of the input mode-cleaner cavity) and the dark fringe to obtain specifications on the spectral densities of the noise sources and specifications on the servo loop gains. These specifications were inputs for the design of the electronics.

The design of an architecture of four entangled loops, together with the knowledge of the interferometer asymmetry, ensures that the laser frequency noise should not show up in the dark fringe, corresponding to the gravitational-wave channel.

IV. CALIBRATIONS OF THE ERROR SIGNALS

In this section we describe the experimental procedure to measure the parameters used to translate the measured error
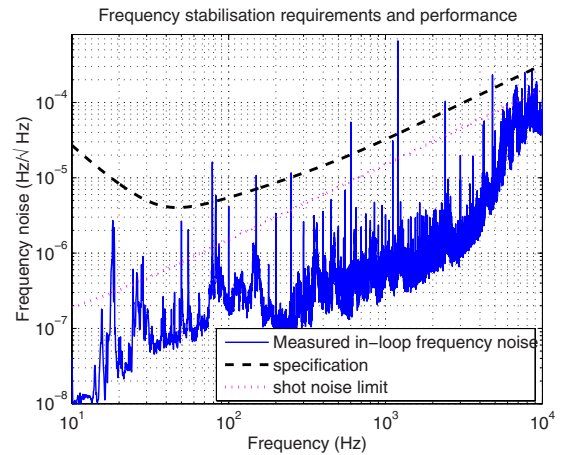

FIG. 2. (Color online) The solid line is the spectral density of the second stage of frequency stabilization error signal; the dotted line is the estimated out-of-loop shot noise stabilization limit; and the dashed line shows the specifications for the error signal of the second stage of laser frequency stabilization.

signal spectra into calibrated data, to be compared with the calculated specifications.

The error and correction signals of the four loops are calibrated. The calibration is supported by analytical models for the Pound-Drever-Hall signals. The entanglement of the loops cross checks the calibration values.

We first calibrated the rigid reference cavity error signal. To this aim, the laser frequency is locked on the input mode-cleaner cavity, all other loops being switched off. The mode-cleaner end mirror position is then swept and the correction signal on the piezoelectric mount of the laser cavity, as well as the Pound-Drever-Hall signal of the rigid reference cavity, is recorded. The shape displays the carrier and the sideband resonances. This calibrates the x axis. The fit of the slope gives a sensitivity of 45×10^{-6} V/Hz and a pole at 250 kHz.

The fit of decay time exponential curves measures the input mode-cleaner pole at 496 Hz [8]. The open loop transfer function of the lock of the laser on the mode cleaner is measured by injecting a perturbation on the error signal and computing the transfer function between the error signal before and after the addition point. Knowing the correction signal calibration and the electronic transfer function, a fit of the open loop transfer function yields the error signal slope, 220×10^{-6} V/Hz.

The correction signal of the second stage of frequency stabilization has the same sensitivity than the input mode-cleaner cavity error signal. The fit of the open loop transfer functions gives a sensitivity of the common mode error signal of 12 V/Hz. The cavity pole of 8 Hz is extracted from a fit of the shape of the transfer function between frequency noise and the common mode error signal for frequencies around the free spectral range [9].

The asymmetry function is measured in the following way. First, the transfer function between the error point of the second stage of frequency stabilization and the dark fringe is measured. This measurement is then corrected from the two frequency dependent signal sensitivities, as well as from the dark fringe loop gain. When the measurement was
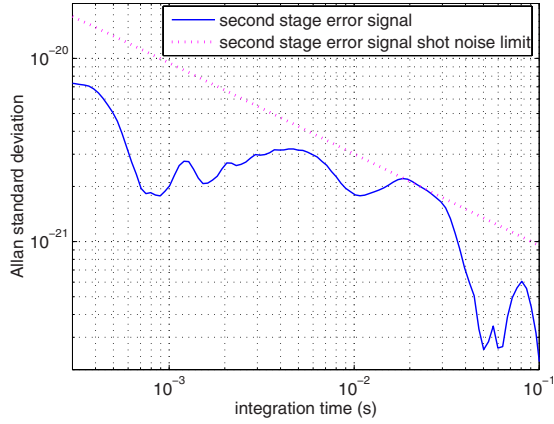
FIG. 3. (Color online) Allan standard deviation, computed from the spectral density of the error signal of the second stage of frequency stabilization.

FIG. 4. (Color online) Estimated fraction of laser frequency noise in the actual dark fringe channel.

done, it was compatible with a zero finesse asymmetry and a pure loss asymmetry. An etalon effect occurs between the two parallel faces of the long cavity input mirrors. This effect is not controlled yet but does not change significantly the specifications for the laser frequency stability.

We now have a design of the frequency stabilization architecture, a measurement of the asymmetry transfer function from laser frequency noise to dark fringe, so we have specifications on the laser frequency noise. With calibrated measurements of the frequency dependent sensitivities of the error signal, we are able to evaluate the performance of the laser frequency stabilization of the Virgo interferometer.

V. PERFORMANCE MEASUREMENT

In this section we report on the obtained laser frequency stability. It is compared with the spectral density noise specification. We show that the laser frequency noise, as measured in loop, does not appear on the dark fringe. The performance is translated into Allan variance measurement so that it can be compared to other oscillators.

The spectral density of the error signal of the second stage of frequency stabilization is recorded while the interferometer is in "science mode" when all control loops are tuned for the best resolution [5]. Figure 2 displays the result from 40 fast Fourier transform (FFT) averages with a Hanning window. The data are calibrated with the measured sensitivity of 12 V/Hz and the pole at 8 Hz. The shot noise level is estimated from the 43 mW incident on the photodiode and the measured sensitivity. The out-of-loop performance cannot be better than the in-loop shot noise limit. The laser linewidth from the estimated shot noise level is 9 mHz.
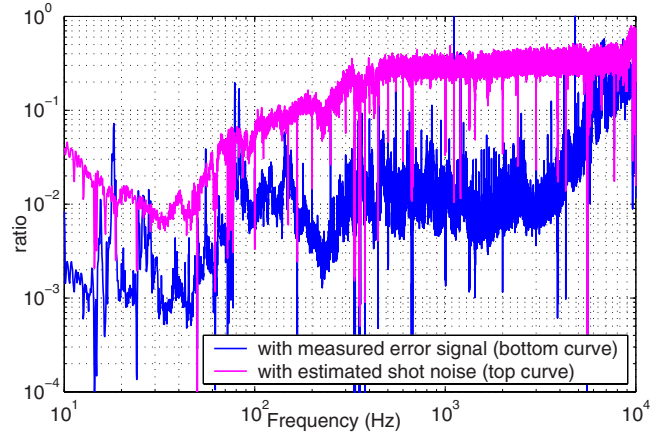
The Allan standard deviation is computed from the spectral density with [10]

$$\sigma_{\bar{y}}^2(\tau) = \int_0^\infty \left(\frac{\tilde{\nu}(f)}{\nu_0}\right)^2 2 \sin^2(\pi\tau f)\left(\frac{\sin \pi\tau f}{\pi\tau f}\right)^2 df.$$

In this calculation, we do not compensate the data for the recycling cavity pole at 8 Hz: the result would be divergent. The relative stability performance is limited by the shot noise, 1.0×10^{-21}, on a 100-ms time scale, as shown in Fig. 3.

The interferometer dark fringe signal is less sensitive to a relative laser frequency noise than to other noise sources. For this, we measured the transfer function between a perturbation in the frequency stabilization error signal and the dark fringe; then we estimated the laser frequency noise contribution with the multiplication of this transfer function by the error signal spectral density. Figure 4 shows that the laser frequency noise should not dominate even when we consider the shot noise contribution of this loop. We do not have at hand an out-of-loop measurement; however, a coherence measurement between the second stage of frequency stabilization error signal and the dark fringe shows that the laser frequency noise indeed does not contribute significantly to the dark fringe.

VI. CONCLUSION

We have shown that the Allan standard deviation of the laser relative frequency noise in the Virgo instrument, measured in loop, is 1.0×10^{-21} on 100 ms. It is limited by the photon shot noise of the error signal. We realized a laser with a frequency stable enough such that the Virgo instrument could measure gravitational waves with its target resolution spectral density of $4.5 \times 10^{-23}/\sqrt{Hz}$ at 350 Hz.

[1] A. Bozzi *et al.*, Rev. Sci. Instrum. **73**, 2143 (2002).
[2] R. V. Pound, Rev. Sci. Instrum. **17**, 490 (1946).
[3] R. W. P. Drever, J. L. Hall, F. V. Kowalsky, J. Hough, G. M. Ford, A. J. Munley, and H. Ward, Appl. Phys. B: Lasers Opt.

31, 97 (1983).
[4] D. Sigg and the LIGO Science Collaboration, Class. Quantum Grav. **23**, S51 (2006).
[5] F. Acernese *et al.*, Class. Quantum Grav. **23**, S63 (2006).

[6] F. Bondu, A. Brillet, F. Cleva, H. Heitmann, M. Loupias, C. Man, H. Trinquet, and The VIRGO Collaboration, Class. Quantum Grav. **19**, 1829 (2002).

[7] K. Numata, A. Kemery, and J. Camp, Phys. Rev. Lett. **93**, 250602 (2004).

[8] The Virgo Collaboration, Appl. Opt. **46**, 3466 (2007).

[9] F. Bondu and O. Debieu, Appl. Opt. **46**, 2611 (2007).

[10] F. Hartmann and F. Stoeckel, J. Phys. (Paris), Colloq. **39**, C1-32 (1978).